This is an accepted manuscript of the following article: Toshinari Mitsuoka, Kenji Hanamura, Noriko Koganezawa, Ruri Kikura-Hnajiri, Yuko Sekino, Tomoaki Shirao. Assessment of NMDA receptor inhibition of phencyclidine analogues using a high-throughput drebrin immunocytochemical assay, *Journal of Pharmacological and Toxicological Methods, 2019,* which has been published in final form at https://doi.org/10.1016/j.vascn.2019.106583

Assessment of NMDA receptor inhibition of phencyclidine analogues using a high-throughput drebrin immunocytochemical assay

Toshinari Mitsuoka[a,c], Kenji Hanamura[a], Noriko Koganezawa[a], Ruri Kikura-Hanajiri[b], Yuko Sekino[c], Tomoaki Shirao[a,*]

[a]Department of Neurobiology and Behavior, Gunma University Graduate School of Medicine, Maebashi 371-8511, Japan

[b]Division of Pharmacognosy, Phytochemistry and Narcotics, National Institute of Health Sciences, Kawasaki 210-9501, Japan

[c]Endowed Laboratory of Human Cell-Based Drug Discovery, Graduate School of Pharmaceutical Sciences, The University of Tokyo, Tokyo 113-0033, Japan

Abbreviated Title: Assessment of NMDA receptor inhibition of phencyclidine analogues

*Corresponding author: Tomoaki Shirao, M.D., Ph.D.

Department of Neurobiology and Behavior, Gunma University Graduate School of

Medicine, 3-39-22, Showa-machi, Maebashi, Gunma 371-8511, Japan

Tel: +81-27-220-8052; Fax: +81-27-220-8053

E-mail: tshirao@gunma-u.ac.jp

Declarations of interest: none

Keywords

dendritic spine; drebrin; high-throughput analysis; immunocytochemistry; NMDA receptor antagonist; phencyclidine; primary neuronal culture; psychoactive substances; synapse

Abbreviations

DAPI, 4',6-diamidino-2-phenylindole, dihydrochloride; DIV, day(s) in vitro; 3-MeO-PCMo, 4-[1-(3-methoxyphenyl)cyclohexyl]morpholine; 3-MeO-PCP, 3-methoxyphencyclidine; NMDA receptor, N-methyl-D-aspartic acid-type glutamate receptor; NPS, new psychoactive substances; PBS, phosphate-buffered saline; PBSA, 3 % bovine serum albumin in PBS; PCP, phencyclidine; S.E.M., standard error of the mean.

Abstract

Introduction: In recent years, new psychoactive substances (NPS) have been widely distributed for abuse purposes. Effective measures to counter the spread of NPS are to promptly legislate them through the risk assessment. Phencyclidine analogues having inhibitory effects toward NMDA receptor (NMDAR) have recently emerged in Japan. Therefore, it is important to establish a high-throughput system for efficiently detecting NPS that can inhibit NMDAR activity. **Methods:** Hippocampal neurons prepared from embryonic rats were incubated in 96-well microplates. After 3 weeks *in vitro*, cultured neurons were preincubated with phencyclidine (PCP) or PCP-analogues, including 3-methoxyphencyclidine (3-MeO-PCP) and 4-[1-(3-methoxyphenyl)cyclohexyl]morpholine (3-MeO-PCMo), and then treated with 100 μM glutamate for 10 min. After fixation, cultured neurons were immunostained with anti-drebrin and anti-MAP2 antibodies. The linear cluster density of drebrin along the dendrites was automatically quantified using a protocol that was originally developed by us. **Results:** The high-throughput immunocytochemical assay, measuring drebrin cluster density of cultured neurons, demonstrated that glutamate-induced reduction of drebrin cluster density in 96-well plates is competitively inhibited by NMDAR antagonist, APV. The reduction was also antagonized by PCP, 3-MeO-PCP and 3-MeO-PCMo. The

inhibitory activity of 3-MeO-PCMo was lower than that of PCP or 3-MeO-PCP, with IC_{50} values of 26.67 μM (3-MeO-PCMo), 2.02 μM (PCP) and 1.51 μM (3-MeO-PCP).

Discussion: The relative efficacy among PCP, 3-MeO-PCP and 3-MeO-PCMo calculated from IC_{50} are similar to those from Ki values. This suggests that the high-throughput imaging analysis is useful to speculate the Ki values of new PCP analogues without performing the kinetic studies.

1. Introduction

New psychoactive substances (NPS) are marketed using terms such as “legal highs” “bath salts” or “research chemicals”; however, they are substances of abuse with effects similar to that of drugs under international control (UNODC, 2017). The emergence of NPS has been reported by > 100 countries and territories worldwide and their distribution has increased the public health concern in many nations. Therefore, it is important to facilitate the accumulation of the relevant data and analysis available on NPS to promptly legislate these substances through a risk assessment process.

NPS with NMDA receptor (NMDAR) inhibitory activity have recently emerged, including methoxethamine and diphenidine (Hondebrink et al., 2017; Kang et al., 2017; Kikura-Hanajiri, 2014; Kikura-Hanajiri, 2017; Roth et al., 2013). Although NMDAR is primarily involved in learning and memory in the central nervous system, if NMDAR activity is reduced, amnesia, perceptual alterations, hallucinations and delusions can occur. This effect involving perceptual and spiritual phenomena can lead to the use of NMDAR inhibitors as abused drugs, with these substances likely having dangerous effects similar to that of narcotics (Morris & Wallach, 2014).

Regarding the detection of NMDAR inhibitory activity, there are two ways in which it can be measured. The first is the calcium imaging method (Ring & Tanso, 2007; Sato et

al., 2016), whereas the second is the displacement assay using tritium labeled MK801 with isotopes (Reynolds, 2001). These assays are useful because of their respective characteristics; however, they cannot directly, simply, or quickly measure NMDAR inhibitory action because of their inability to directly measure the action on NMDAR, their complicated operation, or the use of a radioisotope.

Cultured neurons gradually extend dendrites during incubation and represent matured synapses between neurons; in 3 weeks, the structure called “dendritic spine” having a mushroom-shaped head is completed. In the dendritic spine, drebrin is accumulated at high concentrations with actin filaments, and stabilizes the dynamics of receptors and scaffold proteins in dendritic spines (Sekino et al., 2007; Shirao et al., 2017). Glutamate treatment on neurons induces rapid drebrin exodus from dendritic spines (Sekino et al., 2006; Mizui et al., 2014). Although administered glutamate activates both AMPAR and NMDAR, the drebrin exodus is specifically induced with NMDAR activation, and is quantitative (Koganezawa et al., 2017; Mizui et al., 2014; Sekino et al., 2017).

We have recently developed a high-throughput imaging analysis of the linear density of drebrin clusters along dendrites for detecting synaptic status, which is sensitive enough to detect the effects of glutamate receptor activation on synapses (Hanamura et al.

submitted to the same special issue of *J. Pharmacol. Toxicol. Methods*). In this study, we use this method in the evaluation of the inhibitory activity of two phencyclidine (PCP) analogues, with PCP used as the positive control. The inhibitory activity of 3-methoxyphencyclidine (3-MeO-PCP) and 4-[1-(3-methoxyphenyl)cyclohexyl]morpholine (3-MeO-PCMo) is determined by measuring the reduction in the linear density of drebrin clusters after glutamate stimulation to NMDAR.

2. Methods

*2.1. Animals.*Animal experiments were performed according to the guidelines set by the Animal Care and Experimentation Committee (Gunma University, Showa Campus, Maebashi, Japan) and conformed to NIH guidelines for the use of animals in research. All efforts were made to minimize animal suffering and to reduce the number of animals used. Pregnant Wistar rats were obtained from Charles River Japan Inc. (Yokohama, Japan). Animals were maintained under standard animal facility conditions with free access to food and water.

2.2. Hippocampal neuronal culture. Frozen neurons prepared from the hippocampus of embryonic day 18 rats were seeded on 96-well plates pre-coated with poly-Lysine

(Thermo 96 Well Black Poly Bottom Poly-Lysine, 152037, ThermoFisher Scientific, Waltham, MA, USA) at a density of 3.0×10^4 cells per cm^2 using Neurobasal Medium containing B27 supplement, penicillin / streptomycin and L-alanyl-L-glutamine (Glutamax-I) (ThermoFisher Scientific) and incubated at 37°C, 5% CO_2. At 4 days in vitro (DIV), Cytosine β-D-arabino-furanoside (Sigma, St. Louis, MO, USA) was added to a final concentration of 0.2 μM to reduce the growth of glia. After the neurons were cultured for 21 DIV, they were pharmacologically treated.

2.3. Administration of drugs. PCP, 3-MeO-PCMo, and 3-MeO-PCP (Cayman Chemical, Ann Arbor, MI, USA) were diluted to predetermined concentrations in a 0.1% DMSO solution and administered in cultured neural cells in the prescribed wells of the 96-well plates. Glutamate (Wako Pure Chemical Industries, Ltd., Osaka, Japan) solution was prepared such that the final concentration in the wells was 100 μM and was administered 10 min after the administration of the drug solution. For the experiments to obtain dose response curve of drebrin cluster density, final glutamate concentration was 1, 3, 10, 30, 50 or 100 μM. Some neurons were treated by APV (an NMDAR competitive antagonist, 50, 100 or 500 μM) for 10 min before the glutamate treatments.

2.4. Immunocytochemistry. The cultured neurons were fixed with 4% paraformaldehyde in phosphate buffer. After permeabilization with 0.1% Triton X-100 in phosphate buffered saline (PBS) for 5 min, the neurons were blocked with 3% bovine serum albumin in PBS (PBSA) for 1 h at room temperature (RT), then incubated with primary antibodies overnight at 4°C. Anti-drebrin antibody (mouse monoclonal, M2F6, 1:1) and anti-MAP2 antibody (rabbit polyclonal, 1:2000, Merck Millipore, Darmstadt, Germany) were used as primary antibodies. After washing with PBS, the cells were incubated with secondary antibodies and 4',6-Diamidino-2-Phenylindole, Dihydrochloride (DAPI, 1:1000, ThermoFisher Scientific) for 1 h at RT. Secondary antibodies used were Alexa Fluor 488 donkey anti-mouse IgG (1:250, Jackson ImmunoResearch Laboratories, Inc. West Grove, PA, USA.) and goat Alexa Fluor 594 donkey anti-rabbit IgG (1:250, Jackson ImmunoResearch Laboratories, Inc.).

2.5. Automatic acquisition of images and analysis. The triple-stained images of the hippocampal neural cells cultured in the 96-well plates were automatically acquired (20× lens, numerical aperture 0.45) by using the automatic focus function of an IN Cell Analyzer 2200 (GE Healthcare, Chicago, IL, USA). All of the data were collected at 2048 × 2048 resolution at 16 bits/pixel and a single pixel in the image corresponded to a

325 nm square in the specimen plane. The obtained images were analyzed by IN Cell Developer Toolbox (GE Healthcare) using a newly developed protocol (Hanamura et al. submitted to the same special issue of *J. Pharmacol. Toxicol. Methods*), and quantified the linear density of drebrin clusters along dendrite.

2.6. Statistics. Data were statistically analyzed by *t*-test or Turkey-Kramer's test following ANOVA with p values 0.05 being considered significant (Statcel4 Excel statistics, The publisher OMS Ltd, Tokyo, Japan). All data are presented as mean ± standard error of the mean (S.E.M.). Commercial software (GraphPad Prism8, Graphpad software com, San Diego, CA, USA) was used to draw the dose fitting curve and calculate EC_{50} and IC_{50}.

3. Results

3.1 Glutamate treatment decreased drebrin cluster density through NMDAR activation

First, we determined the effects of glutamate on drebrin cluster density using our high-throughput imaging system. Rat hippocampal cultured neurons were treated by several concentration of glutamate (1 μM, N = 61; 3 μM, N = 97; 10 μM, N = 88; 30 μM, N = 97; 50 μM, N = 20; 100 μM, N = 106) at 21 days in vitro (DIV). After immunocytochemistry, image acquisitions and analysis were done by automatically.

Obtained glutamate dose response curve of drebrin cluster density is shown in Figure 1A. EC_{50} was 10.4 μM with the 95% confidence interval (CI) ranging from 6.29 μM to 17.4 μM.

We also determined that this decrease of drebrin cluster density by glutamate stimulation is blocked by applying APV (50 μM, N = 4; 100 μM, N = 7; 500 μM, N = 6) to some extent (Figure 1B). The results indicate that our high-throughput imaging system is able to detect the reduction of drebrin cluster density by glutamate stimulation and its blockage by an NMDAR competitive antagonist.

3.2 Inhibitory effect of PCP, 3-MeO-PCMo and 3-MeO-PCP on glutamate-induced decrease of drebrin cluster density.

First, we determined to what extent the density of the drebrin clusters would be reduced using 100 μM glutamate (control; N = 95, glutamate 100 μM; N = 77). As shown in Figure 2A, 100 μM glutamate reduced the drebrin cluster density approximately 40% of the control group (control; 0.538 ± 0.0143, 100 μM glutamate; 0.319 ± 0.0035).

We then investigated the inhibitory effect of PCP, a noncompetitive antagonist of NMDAR, on the reduction in the density of the drebrin clusters by NMDAR stimulation with glutamate (0–10 μM, N = 18). The average inhibition rate of each administration

group against the control group was calculated to analyze the dose-dependent effects. Figure 2B shows that PCP significantly inhibited the reduction of drebrin clusters at a concentration of ≥1 μM by NMDAR stimulation of the 100 μM glutamate, and PCP inhibited the reduction of the drebrin clusters in a dose-dependent manner.

Moreover, we investigated the inhibitory action of PCP analogues, 3-MeO-PCP and 3-MeO-PCMo, in the similar manner (0–10 μM, 3-MeO-PCP; N = 29, 3-MeO-PCMo; N = 30). Figure 2C shows that 3-MeO-PCP significantly inhibited the reduction of the drebrin clusters by 100 μM glutamate at a concentration of ≥333 nM. Figure 2D shows that 3-MeO-PCMo inhibited significantly that at a concentration of ≥3.33 μM. In addition, both 3-MeO-PCP and 3-MeO-PCMo inhibited the reduction of the drebrin clusters in a dose-dependent manner.

3.3 IC50 values of PCP, PCP, 3-MeO-PCMo and 3-MeO-PCP

To increase the quantitative reliability of the analysis, the dose-effect curve was created, which was curve-fitted based on a theoretical formula (Gesztelyi et al., 2012; Gadagkar & Call, 2015) to evaluate the difference by comparing the actions of PCP and 3-MeO-PCP or 3-MeO-PCMo. In addition, the inhibitor concentration that reduces activity by half maximal inhibitory concentration (IC_{50}) values of each substance were

measured. Figure 3 shows that the inhibitory activity of 3-MeO-PCP was comparable to that of PCP and the inhibitory activity of 3-MeO-PCMo was lower than that of PCP, with IC_{50} values of PCP = 2.02 μM (95%CI 1.39-2.97), 3-MeO-PCP =1.51 μM (95%CI 1.16 -1.99), 3-MeO-PCMo = 26. 7 μM (95%CI 20.0-37.3).

4. Discussion

In this study, we quantified the IC_{50} values of PCP, 3-MeO-PCP and 3-MeO-PCMo by measuring drebrin cluster density using a high-throughput imaging analysis that we recently developed, and demonstrated that the order of inhibitory activity was 3-MeO-PCP > PCP > 3-MeO-PCMo. In this part, we discuss the usefulness of measuring drebrin cluster density to calculate IC_{50} and speculate Ki values of PCP analogues using the high-throughput analysis system. Furthermore, we discuss its use in safety pharmacology study from the view of pharmacodynamic of NMDAR antagonism.

NMDAR is composed of four subunits, comprising two sets of heterodimers, namely NR1 and NR2. NMDAR has a PCP binding site. PCP, MK801 or ketamine binds to NMDAR, exerting their effect by inhibiting NMDAR activity (Dingledine et al., 1999; Paoletti & Neyton, 2007; Lee et al., 2014).

PCP acts as a dose-dependent NMDAR inhibitor by blocking the open channel pore, and has a high affinity for the PCP binding site of NMDAR (Wallach & Brandt, 2018; Wallach 2014; Lodge & Mercier, 2015). In recent studies involving binding assays toward NMDAR, inhibition constant (Ki) values of PCP and 3-MeO-PCP have been reported as 57.9 nM and 38.1 nM, respectively (Wallach, 2014). In contrast, the Ki value of PCP and 3-MeO-PCMo have been reported as 22.1 nM and 252.9 nM, respectively (Colestock et al., 2018). The affinity ratio against PCP from the above Ki values were calculated. The results were 3-MeO-PCP = 0.73 (recalculation from Ki value of "Wallach 2014"), 3-MeO-PCMo = 11.4 (recalculation from Ki value of "Colestock et al., 2018") as PCP = 1. In summary, the order of affinity appears to be comparable to that of their PCP counterparts, with 3-MeO-PCP > PCP > 3-MeO-PCMo.

The relationship between Ki and IC_{50} varies. However, when a group of inhibitory compounds have an identical mechanism of action, a direct comparison of the IC_{50} values among them suffices to determine the relative efficacy (Cheng & Prusoff, 1973; Cer et al., 2009). PCP and other high-affinity NMDAR antagonists have been suggested to have a similar inhibitory mechanism of NMDAR (Lodge & Mercier, 2015). Therefore, the potency ratio against PCP from the IC_{50} values obtained in this study were calculated, the results were 3-MeO-PCP = 0.75, 3-MeO-PCMo = 13.2 as PCP = 1. Thus, the relative

efficacy among PCP, 3-MeO-PCP and 3-MeO-PCMo calculated from IC_{50} are similar to those from Ki values. Consequently, the IC_{50} value obtained from this system reflects NMDAR antagonist action and can be used for the pharmacological evaluation (toxicity evaluation) of NPS with NMDAR inhibitory activity.

When the Ki values of NPSs are required, it may be impractical to perform the kinetic studies required to determine the Ki for each (Cheng & Prusoff, 1973). However, if the Ki of one compound that have a similar inhibitory mechanism, the Ki values can be calculated from IC_{50}. Considering that this high-throughput analysis can efficiently provide related data at varying drug concentrations with one measurement, this system is useful as an evaluation system for detecting the inhibitory action on the glutamate NMDAR for the risk assessment of NPS.

Some studies have reported that the *in vitro* potencies of NMDAR antagonists closely correlate with the affinities reported by PCP binding assays, with the PCP analogues discrimination in animal models correlating well with the affinities toward the PCP site of NMDAR (Lodge & Mercier, 2015). However, the correlating potency of NMDAR antagonists with dysphoric and psychotomimetic potency in humans was more tenuous (Lodge & Mercier, 2015). If neurons derived from human iPS cells are subjected to the

high-throughput drebrin immunocytochemical assay in future studies, accurate interpolation of toxicity of these substances to humans may be possible.

In addition, this evaluation system for detecting the inhibitory action on the glutamate NMDAR may be applied to drug development related to neuroprotective effects. The excitotoxicity of NMDAR is a target for drug development toward a wide variety of neurodegenerative disorders, such as Alzheimer's disease, Parkinson's disease, Huntington's disease, multiple sclerosis, amyotrophic lateral sclerosis (ALS), neuropathic pain, glaucoma and vascular dementia (Couratier et al., 1996; Lipton, 2006; Rogawski & Wenk, 2003; Zurakowski et al., 1998). In the subsequent safety pharmacology, it is important to predict mechanism-based pharmacological action, because animal tests have limitations on detecting symptoms like amnesia and hallucination caused by NMDAR antagonism. Thus, our evaluation system can be used for drug discovery and safety pharmacology.

Especially, the pharmacodynamic data play an important role when the consideration of initial dose in a first-in-human clinical trial (European Medicines Agency, 2017). The prediction of pharmacological actions based on the characteristics of NMDAR, such as cellular response consequent to the interaction with NMDAR, duration and reversibility of effect, and dose-response relationships, would be useful for predicting species

differences in pharmacology, effects of genetic polymorphisms, and drug interactions.

In vitro systems can be used in supportive studies to obtain a profile of the activity of the substance under the ICH S7A guidelines (ICH, 2000). The present immunocytochemical assay system is a robust analysis for NMDAR activity with high reproducibility, and does not require any special skills compared with electrophysiological method for detecting NMDAR activity. However, in terms of the limitation of our system in broad applicability to drug safety study use, our system can detect inhibitory activity of NMDAR but not other types of receptors. After a greater evaluation of central nervous system (CNS) and non-CNS drugs is performed using our system, ambiguities on the scope of applicable substances and the magnitude of false negative and/or false positive will be clarified.

Taken together, this system might be used as a part of CNS safety pharmacology in the future.

Author Contributions

T.M., K.H., and N.K. performed experiments and data analysis. T.M., K.H., N.K., R.H., Y.S., and T.S. discussed the results and commented on the manuscript. T.M., K.H., N.K., R.H., Y.S. and T.S. designed the experiments and wrote the manuscript.

Acknowledgements

We thank Ms. Kazumi Kamiyama and Ms. Natsume Tanaka for their technical assistance.

This work was supported by JSPS KAKENHI Grants Number JP17H03557 and JP15K14344 to TS and Japan Agency for Medical Research and Development (AMED) under Grant Number JP17bk0104077, JP18bk0104077 to TS.

References

Cer, R.Z., Mudunuri, U., Stephens, R., & Lebeda, F.J. (2009). IC50-to-Ki: a web-based tool for converting IC50 to Ki values for inhibitors of enzyme activity and ligand binding. *Nucleic Acids Research. 1(37)*: W441–W445. https://doi.org/10.1093/nar/gkp253.

Cheng, Y., & Prusoff, W.H. (1973). Relationship between the inhibition constant (KI) and the concentration of inhibitor which causes 50 per cent inhibition (I50) of an enzymatic reaction. *Biochemical Pharmacology*, *22(23),* 3099-3108. https://doi.org/10.1016/0006-2952(73)90196-2.

Colestock, T., Wallach, J., Mansi, M., Filemban, N., Morris, H., Elliott, S.P., Westphal, F., Brandt, S.D., & Adejare, A. (2018). Syntheses, analytical and pharmacological characterizations of the 'legal high' 4-[1-(3-methoxyphenyl)cyclohexyl]morpholine (3-MeO-PCMo) and analogues. *Drug Testing and Analysis*, *10,* 272-283. https://doi.org/10.1002/ dta. 2213.

Couratier, P., Lesort, M., Sindou, P., Esclaire, F., Yardin, C., & Hugon, J. (1996). Modifications of neuronal phosphorylated tau immunoreactivity induced by NMDA toxicity. *Molecular and Chemical Neuropathology. 27*, 259−273. https://link.springer.com/content/pdf/10.1007%2FBF02815108.pdf.

Dingledine, R., Borges, K., Bowie, D., & Traynelis, S. (1999). The glutamate receptor ion channels. *Pharmacological Reviews, 51 (1),* 7-62. http://pharmrev.aspetjournals.org/content/51/1/7.

European Medicines Agency. (2017). Guideline on strategies to identify and mitigate risks for first-in-human and early clinical trials with investigational medicinal products. https://www.ema.europa.eu/en/news/revised-guideline-first-human-clinical-trials.

Gadagkar, S., & Call, G. (2015). Computational tools for fitting the Hill equation to dose–response curves. *Journal of Pharmacological and Toxicological Methods, 71*, 68–76. https://doi.org/10.1016/j.vascn.2014.08.006.

Gesztelyi, R., Zsuga, J., Kemeny-Beke, A., Varga, B., Juhasz, B., & Tosaki, A. (2012). The Hill equation and the origin of quantitative pharmacology. *Archive for History Exact Science. 66,* 427–438. https://doi.org/10.1007/s00407-012-0098-5.

Hondebrink, L., Kasteel, E., Tukker, A., Wijnolts, F., Verboven, A., & Westerink, R. (2017). Neuropharmacological characterization of the new psychoactive substance methoxetamine. *Neuropharmacology, 123, 1,* 1-9. https://doi.org/10.1016/j.neuropharm.2017.04.035.

ICH. (2000). International Council for Harmonization of technical requirements for pharmaceuticals for human use S7A: safety pharmacology studies for human pharmaceuticals. https://www.ich.org/products/guidelines.html.

Kang, H., Park, P., Bortolotto, Z.A., Brandt, S.D., Colestock, T., Wallach, J., Collingridge, G.L., & Lodge, D. (2017). Ephenidine: A new psychoactive agent with ketamine-like NMDA receptor antagonist properties. *Neuropharmacology,112,* Part A, 144-149. https://doi.org/10.1016/j.neuropharm.2016.08.004.

Kikura-Hanajiri, R., Uchiyama, N., Kawamura, M., & Goda, Y. (2014). Changes in the prevalence of new psychoactive substances before and after the introduction of the generic scheduling of synthetic cannabinoids in Japan. *Drug Testing and Analysis,6,* ,832-839. https://do.org/10.1002/dta.1584

Kikura-Hanajiri, R. (2017). Changes in the prevalence substances and their legal status in Japan. *Folia Pharmacologica Japonica., 150,* 1-6. https://doi.org/10.1254/fpj.150.129.

Koganezawa, N., Hanamura, K., Sekino, Y., & Shirao, T. (2017). The role of drebrin in dendritic spines. *Molecular and Cellular Neuroscience, 84,* 85-92. https://doi.org/10.1016/j.mcn.2017.01.004.

Lee, C.H., Lü, W., Michel, J.C., Goehring, A., Du, J., & Song, X. (2014). NMDA

receptor structures reveal subunit arrangement and pore architecture. *Nature, 511,* 191-197.

Lipton, S.A. (2006). Paradigm shift in neuroprotection by NMDA receptor blockade: Memantine and beyond. *Nature Reviews/Drug discovery, 5,* 160-170. https://doi.org/10.1038/nrd1958.

Lodge, D., & Mercier, M.S. (2015). Ketamine and phencyclidine: the good, the bad and the unexpected. *British Journal of Pharmacology, 172,* 4254–4276. https://doi.org/10.1111/bph.13222.

Mizui, T., Sekino, Y., Yamazaki, H., Ishizuka, Y., Takahashi, H., Kojima, N., Kojima, M., & Shirao, T. (2014). Myosin II ATPase activity mediates the long-term potentiation-induced exodus of stable F-actin bound by drebrin A from dendritic spines. *PLoS One, 9,* e85367. https://doi.org/10.1371/journal.pone.0085367.

Morris, H., & Wallach, J. (2014). From PCP to MXE: A comprehensive review of the non-medical use of dissociative drugs. *Drug Testing and Analysis, 6,* 614-632. https://doi.org/10.1002/dta.1620.

Paoletti, P., & Neyton, J. (2007). NMDA receptor subunits-function and pharmacology. *Current Opinion in Pharmacology, 7(1),* 39-47. https://doi.org/10.1016/j.coph.2006.08.011.

Reynolds, I.J. (2001). [^{3}H] (+) MK801 radioligand binding assay at the N-methyl-D-aspartate receptor. *Current Protocol Pharmacology, Unit 1-20,* 2001, 1-8. https//doi. org/10.1002/0471141755.ph0120s11.

Ring, A., & Tanso, R. (2007). Measurements with fluorescent probes in primary neural cultures; improved multiwell techniques. *Journal of Pharmacological and Toxicological Methods* 56, 300−307. https://doi.org/10.1016/j.vascn.2007.05.004.

Rogawski, M.A. & Wenk, G.L. (2003). The neuropharmacological basis for the use of memantine in the treatment of Alzheimer's disease. *CNS Drug Reviews.* 9, 275−308. https://doi.org/10.1111/j.1527-3458.2003.tb00254.x.

Roth, B., Gibbons, S., Arunotayanun, W., Huang, X., Setola, V., & Treble, R. (2013). The ketamine analogue methoxetamine and 3- and 4-methoxy analogues of phencyclidine are high affinity and selective ligands for the glutamate NMDA. *Les Iversen published.* https://doi.org/10.1371/journal.pone.0059334.

Sato, K., Takahashi, K., Shigemoto-Mogami, Y., Chujo, K., & Sekino, Y. (2016). Glypican 6 enhances N-methyl-D-aspartate receptor function in human-induced pluripotent stem cell-derived neurons. *Frontiers in Cellular Neuroscience, 10(259).* https://doi.org/10.3389/fncel.2016.00259.

Sekino, Y., Koganezawa, N., Mizui, T., & Shirao, T. (2017). Role of Drebrin in Synaptic

Plasticity, *Advances in Experimental Medicine and Biology-Drebrin, 1006* (183–201). Tokyo: Springer. https://doi.org/10.1007/978-4-431-56550-5_11.

Sekino, Y., Kojima, N., & Shirao, T. (2007). Role of actin cytoskeleton in dendritic spine morphogenesis. *Neurochemistry International, 51,* 92-104. https://doi.org/10.1016/j.neuint.2007.04.029.

Sekino, Y., Tanaka, S., Hanamura, K., Yamazaki, H., Sasagawa, Y., Xue, Y., Hayashi, K., & Shirao, T. (2006). Activation of N-methyl-d-aspartate receptor induces a shift of drebrin distribution: Disappearance from dendritic spines and appearance in dendritic shafts. *Molecular Cellular Neuroscience, 31,* 493-594. https://doi.org/10.1016/ j.mcn.2005.11.003.

Sekino, Y., Koganezawa, N., Mizui, T., & Shirao, T. (2017). Role of Drebrin in Synaptic Plasticity, *Advances in Experimental Medicine and Biology-Drebrin, 1006* (183–201). Tokyo: Springer. https://doi.org/10.1007/978-4-431-56550-5_11.

Shirao, T., Hanamura, K., Koganezawa, N., Ishizuka, Y., Yamazaki, H., & Sekino, Y. (2017). The role of drebrin in neurons. *Journal of Neurochemistry, 141(6),* 819-834. https://doi.org/10.1111/jnc.13988.

UNODC. (2017). Global synthetic drugs assessment-amphetamine-type stimulants and new psychoactive substances. Vienna: United Nations Office on Drugs and Crime.

https://www.unodc.org/unodc/en/scientists/global-synthetic-drugs-assessment-2017.html. Accessed October 2017.

Wallach, J., & Brandt, S.D. (2018). Phencyclidine-Based New Psychoactive Substances. *New Psychoactive Substances* (pp. 261-303), Springer International Publishing AG. https://doi.org/10.1007/164_2018_124.

Wallach, J. (2014). Structure activity relationship (SAR) studies of arylcyclohexylamines as N-methyl-D-aspartate receptor antagonists. PhD dissertation. University of the Sciences, Philadelphia.

Zurakowski, D., Kvorwerk, C., Gorlab, M., Kanellopoulosc, A.J., Chaturvedic,N., Grosskreutzc, C.L., Lipton, S.A., & Dreyer, E.B.(1998). Nitrate therapy may retard glaucomatous optic neuropathy, perhaps through modulation of glutamate receptors. *Vision Research. 38*, 1489−1494. https://doi.org/10.1016/S0042-6989(98)00003-0.

Figure legends

Figure 1. Glutamate dose response curve of drebrin cluster density. (A) Drebrin cluster density were normalized by the average density of control group (N = 61). The dose response curve were fitted based on the theoretical formula: Y = Bottom + (1 − Bottom) / (1+10^ ((LogEC_{50}−X) * HillSlope)). Cultured neurons at DIV 21 were treated with several dose of glutamate (1, 3, 10, 30, 50 or 100 μM) for 10 min. Each dot indicates individual values (1 μM, N = 61; 3 μM, N = 97; 10 μM, N = 88; 30 μM, N = 97; 50 μM, N = 20; 100 μM, N = 106). (B) To examine the effect of an NMDAR antagonist, some neurons were treated with APV (50 μM, N = 4; 100 μM, N = 7; 500 μM, N = 6) 10 min prior to the glutamate treatments. The dose response curve for APV (0 μM) is the same as that of Figure 1A. Data are presented as mean ± S.E.M.

Figure 2. Effects of drug treatments on the drebrin cluster density. (A) Effects of glutamate treatment. Upper panel shows representative images of neurons (MAP2 (red), drebrin clusters (green or monochrome) compared 100 μM glutamate administration to naive control. Lower panel shows quantitative analysis of drebrin cluster density (/μm dendrite). Data are presented as mean ± S.E.M. * $p < 0.05$, t-test. (B) Inhibitory potency

of PCP on the reduction of drebrin clusters by glutamate. Administration group (0.1 nM-10 μM) was normalized by assuming that the average value of the control group was 100%, and that the average value of the 100 μM glutamate administration group was 0%. Administration groups at 1 μM or more significantly inhibited the reduction of drebrin clusters. Values are expressed as mean ± S.E.M., * $p < 0.05$ vs control by Turkey-Kramer's test. (C) Inhibitory potency of 3-MeO-PCP on the reduction of drebrin clusters by glutamate. Administration group (0.1 nM-10 μM) was normalized by assuming that the average value of the control group was 100%, and that the average value of the 100 μM glutamate administration group was 0%. Administration groups of 3-MeO-PCP at 333 nM or more significantly inhibited the reduction of drebrin clusters. Values are expressed as mean ± S.E.M., * $p < 0.05$ vs control by Turkey-Kramer's test. (D) Inhibitory potency of 3-MeO-PCMo on the reduction of drebrin clusters by glutamate. Administration group (0.1 nM-10 μM) was normalized by assuming that the average value of the control group was 100%, and that the average value of the 100 μM glutamate administration group was 0%. Administration groups of 3-MeO-PCMo at 3.33 μM or more significantly inhibited the reduction of drebrin clusters. Values are expressed as mean ± S.E.M., * $p < 0.05$ vs control by Turkey-Kramer's test. Scale bars, 20 μm in A, 10 μm in B, C and D.

Figure 3. Comparison of inhibitory potencies of PCP, 3-MeO- PCP and 3-MeO-PCMo on the reduction of drebrin clusters by glutamate. Each administration group (0.1 nM-10 μM) was normalized by assuming that the average value of the control group was 0%, and that the variation from average value of 100 μM glutamate administration group to the average value of the control group was 100%. Dose response curve was fitted based on the theoretical formula. In addition, IC_{50} were calculated by fitting curves. IC_{50} of PCP, 3-MeO-PCP and 3-MeO-PCMo were 2.02 μM, 1.51 μM and 26.7 μM, respectively. Values are expressed as mean ± S.E.M.

A

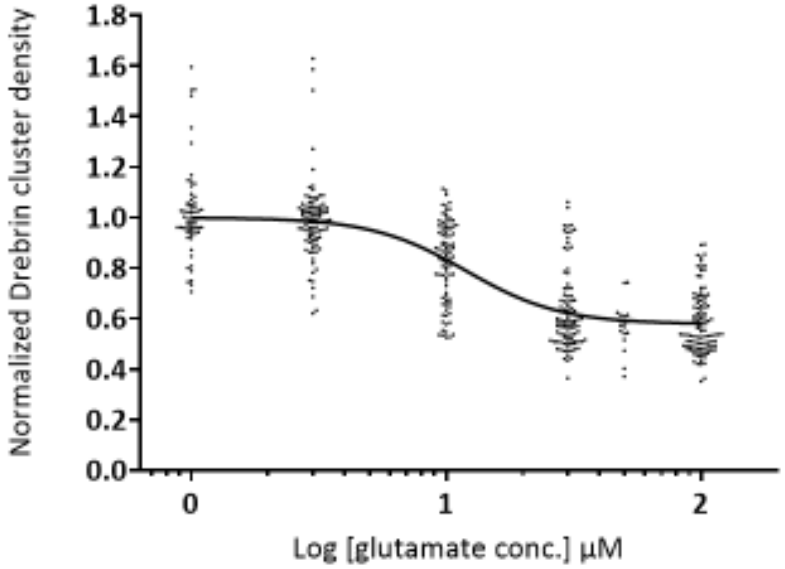
Normalized Drebrin cluster density
1.8
1.6
1.4
1.2
1.0
0.8
0.6
0.4
0.2
0.0
0
1
2
Log [glutamate conc.] μM

B

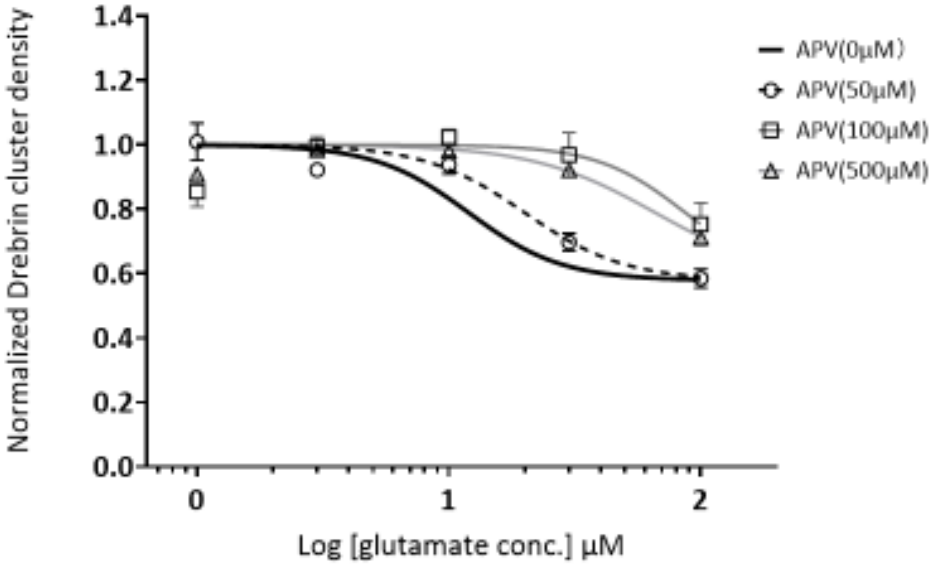
Normalized Drebrin cluster density
1.4
1.2
1.0
0.8
0.6
0.4
0.2
0.0
0
1
2
Log [glutamate conc.] μM
APV(0μM)
APV(50μM)
APV(100μM)
APV(500μM)

Figure 1

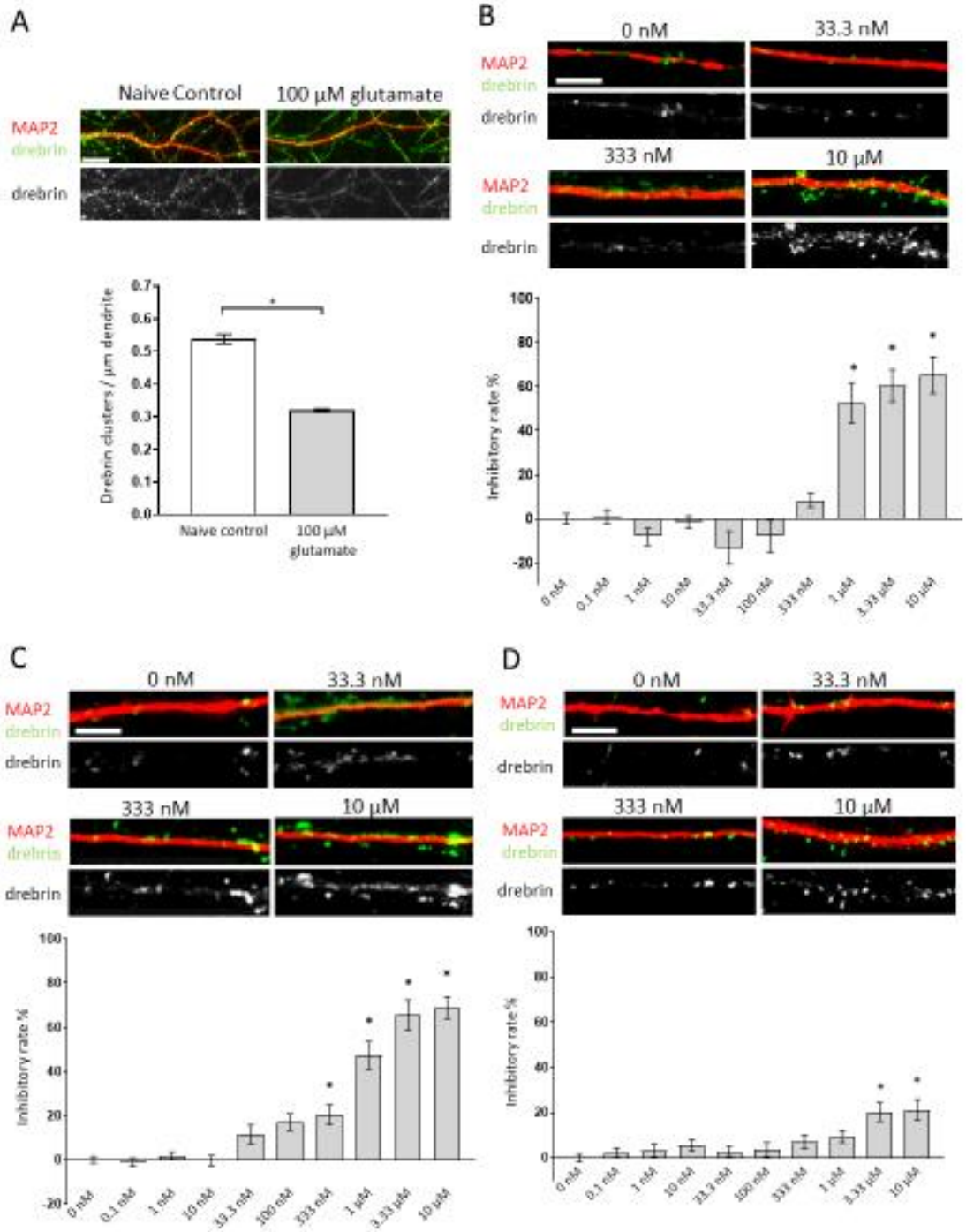
A
Naive Control
100 μM glutamate
MAP2
drebrin
drebrin
Drebrin clusters / μm dendrite
Naive control
100 μM glutamate
B
0 nM
33.3 nM
333 nM
10 μM
MAP2
drebrin
drebrin
Inhibitory rate %
C
0 nM
33.3 nM
333 nM
10 μM
MAP2
drebrin
drebrin
Inhibitory rate %
D
0 nM
33.3 nM
333 nM
10 μM
MAP2
drebrin
drebrin
Inhibitory rate %

Figure 2

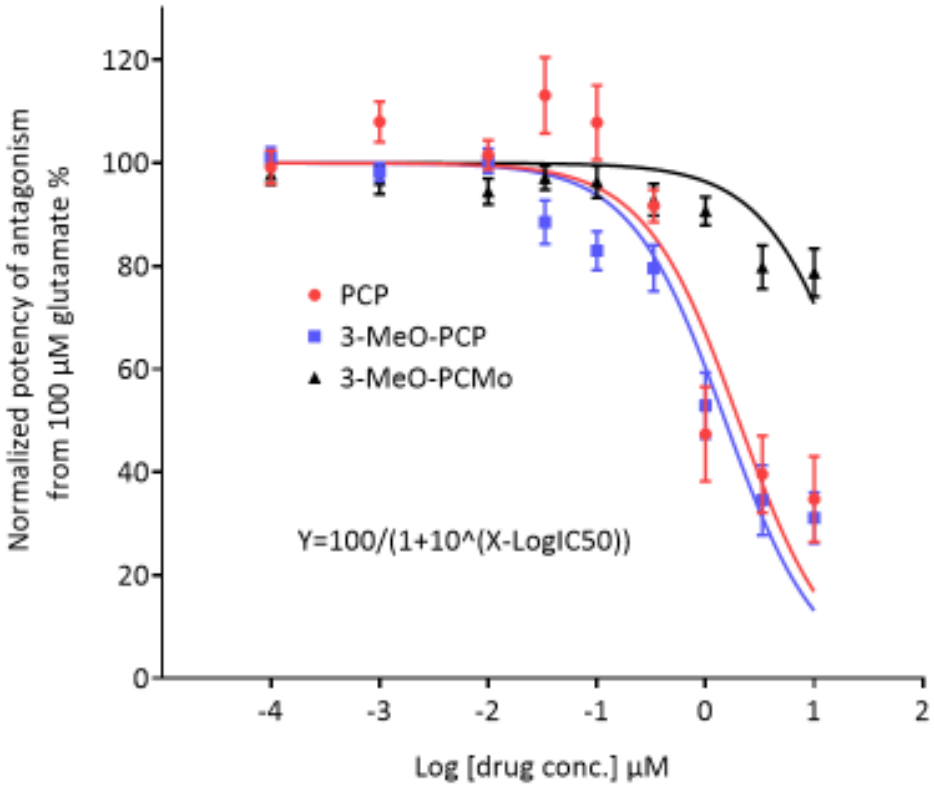
Normalized potency of antagonism from 100 µM glutamate %
120
100
80
60
40
20
0
-4
-3
-2
-1
0
1
2
Log [drug conc.] µM
PCP
3-MeO-PCP
3-MeO-PCMo
Y=100/(1+10^(X-LogIC50))

Figure 3